Recombinant Protein-*co*-PEG Networks as Cell-Adhesive and Proteolytically Degradable Hydrogel Matrixes. Part II: Biofunctional Characteristics

Simone C. Rizzi,[†,‡,#] Martin Ehrbar,[‡,¶] Sven Halstenberg,[§,¶] George P. Raeber,[†,⊥,¶] Hugo G. Schmoekel,[∥] Henri Hagenmüller,[†] Ralph Müller,[†] Franz E. Weber,[‡] and Jeffrey A. Hubbell*[,∥]

Institute for Biomedical Engineering, Swiss Federal Institute of Technology and University of Zurich, Zurich, Switzerland, Department of Cranio-Maxillofacial Surgery, University Hospital Zurich, Zurich, Switzerland, Institute of Pathology, Johannes Gutenberg University, Mainz, Germany, and Laboratory for Regenerative Medicine and Pharmacobiology, Institute of Bioengineering and Institute for Chemical Sciences and Engineering, Ecole Polytechnique Fédérale de Lausanne (EPFL), Lausanne, Switzerland

Received May 23, 2006; Revised Manuscript Received September 4, 2006

We present here the biological performance in supporting tissue regeneration of hybrid hydrogels consisting of genetically engineered protein polymers that carry specific features of the natural extracellular matrix, cross-linked with reactive poly(ethylene glycol) (PEG). Specifically, the protein polymers contain the cell adhesion motif RGD, which mediates integrin receptor binding, and degradation sites for plasmin and matrix-metalloproteinases, both being proteases implicated in natural matrix remodeling. Biochemical assays as well as in vitro cell culture experiments confirmed the ability of these protein-PEG hydrogels to promote specific cellular adhesion and to exhibit degradability by the target enzymes. Cell culture experiments demonstrated that proteolytic sensitivity and suitable mechanical properties were critical for three-dimensional cell migration inside these synthetic matrixes. In vivo, protein-PEG matrixes were tested as a carrier of bone morphogenetic protein (rhBMP-2) to heal critical-sized defects in a rat calvarial defect model. The results underscore the importance of fine-tuning material properties of provisional therapeutic matrixes to induce cellular responses conducive to tissue repair. In particular, a lack of rhBMP or insufficient degradability of the protein-PEG matrix prevented healing of bone defects or remodeling and replacement of the artificial matrix. This work confirms the feasibility of attaining desired biological responses in vivo by engineering material properties through the design of single components at the molecular level. The combination of polymer science and recombinant DNA technology emerges as a powerful tool for the development of novel biomaterials.

Introduction

In one approach to tissue repair, a provisional extracellular matrix is delivered in situ to serve as a temporary scaffold that must either contain suitable cell types for tissue repair or recruit cells from the surrounding tissue to the site of injury.[1,2] Remodeling and eventual resorption of the matrix should preferably occur in spatial and temporal synchrony with cellular infiltration and tissue formation.[3] Natural matrixes such as collagen and fibrin meet these requirements as they are resorbed by cell-mediated mechanisms, i.e. pericellular proteolytic degradation.[4−8] Natural materials thus represent the most common and most useful matrixes for therapeutic tissue regeneration to date.[9] However, the wide range of clinical applications for such biomaterials requires better and more flexible control over material properties, so that these materials can be tailored individually toward specific medical needs.[10−13] In addition, the risks associated with human- or animal-derived products render nonautologous matrix materials nonideal for clinical use in general.[14,15] Therefore, the goal of this and earlier studies was to find synthetic analogues of natural extracellular matrix materials that would be amenable to better control of material and biological properties without resorting to natural proteins.[12,13]

Specifically, our aim was to confer two key features of natural matrixes to synthetic or biosynthetic materials: (i) the display of adhesion sites for cell attachment[16,17] and (ii) proteolytic degradability and matrix remodeling,[18−21] both properties that are essential to enable three-dimensional (3D) cell migration within the matrix.[22] So far, material sensitivity to specific cellular activity in the form of cell-mediated proteolysis has been conferred to only few synthetic matrixes.[23−26] Degradation of synthetic materials is more commonly achieved merely by cell-independent mechanisms, such as passive hydrolysis under physiological conditions.

An abundant range of biological signals can be incorporated in synthetic biomaterials as shown here and elsewhere,[27] including the delivery of bone morphogenetic protein (BMP-2) for the regeneration of bone. Proteolytically sensitive synthetic materials have successfully induced the formation of new blood

* Correspondence should be addressed to Prof. Jeffrey A. Hubbell. Telephone: +41 21 693 9681. Fax: +41 21 693 9665. E-mail: jeffrey.hubbell@epfl.ch.

† Swiss Federal Institute of Technology and University of Zurich.

‡ University Hospital Zurich.

Present address: Institute of Health and Biomedical Innovation, Queensland University of Technology (QUT), Brisbane, Australia.

§ Johannes Gutenberg University.

¶ These authors contributed equally.

⊥ Present address: Institute Straumann, Division Products, Basel, Switzerland.

∥ Ecole Polytechnique Fédérale de Lausanne (EPFL).

10.1021/bm060504a CCC: $33.50
Published on Web 10/03/2006

Table 1. Hydrogel Compositions and Properties[a]

hydrogel compositions		hydrogel properties	
protein polymer	dry mass, % (w/v)[d]; r = SH/VS[e]	G' (Pa)[d]	RGD/plasmin/MMP (mM)[g]
degradable dimer	5.5%; $r = r_{opt} = 1$	69 ± 21	1.41 ± 0.11
(MW 11812 Da)[b]	7.5%; $r = r_{opt} = 1$	294 ± 59	2.00 ± 0.10
(SH = 5)[c]	9.5%; $r = r_{opt} = 1$	577 ± 51	2.43 ± 0.12
degradable tetramer	5.5%; $r = r_{opt} = 1.1$	119 ± 23	2.18 ± 0.06
(MW 20310 Da)	7.5%; $r = r_{opt} = 1.1$	455 ± 60	2.98 ± 0.068
(SH = 9)	9.5%; $r = r_{opt} = 1.1$	925 ± 93	3.63 ± 0.06
nondegradable dimer	5.5%; $r = r_{opt} = 1.2$	345 ± 30	2.37 ± 0.03
(MW 11548 Da)	7.5%; r = $r_{opt} = 1.2$	659 ± 21	2.96 ± 0.07
(SH = 5)	9.5%; $r = r_{opt} = 1.2$	1187 ± 89	3.44 ± 0.24
	9.5%; $r = 1$	633 ± 29	2.42 ± 0.05
nondegradable tetramer	9.5%; $r = 1$	2253 ± 204	4.70 ± 0.14
(MW 19783 Da)			
(SH = 9)			

[a] Protein polymers were cross-linked with PEG-di-VS, MW 6000 (Da). [b] Average of molecular weights (MW) of protein polymers measured by TOF-Maldi and electrospray mass spectroscopy.[32] [c] Number of thiols present in the protein polymers. [d] Total solid percent in hydrogels before swelling. [e] Stoichiometric molar ratio (r) of protein thiols (SH) and vinyl sulfone groups (VS) of PEG6000, r_{opt} stoichiometric molar ratio yielding optimal macroscopic hydrogel properties (maximal values of elastic shear modulus G' and minimal values of mass swelling Q_m) determined by Rizzi and Hubbell.[32] [f] Elastic shear moduli (G') of swollen hydrogel disks (PBS, 10 mM, pH 7.4) measured as previously described[32](Average of $n \geq 3 \pm$ SD). [g] Concentration of cell-binding sites (RGD) and protease degradation substrates (for plasmin and MMP) calculated in swollen hydrogels (PBS, 10 mM, pH 7.4) and from the amount of protein polymer employed to form the different gels (Average of $n \geq 3 \pm$ SD).

vessels by providing vascular endothelial growth factor (VEGF).[26,28] Based on these examples, our intention was to develop (bio)synthetic matrixes capable of being remodeled and transformed into target tissue in spatial and temporal synchrony with cellular ingrowth. As a result, exogenous biological signals that can be incorporated within the matrixes are retained and presented during the process of tissue regeneration only.[27,28]

The particular materials presented here belong to a range of two-component hybrid hydrogels based on poly(ethylene glycol) and biomolecules introduced by West and Hubbell to mimic key features of ECM within synthetic materials.[23] The present approach differs substantially from earlier PEG-based matrixes[23,25−27,29−31] in that, here and elsewhere,[24,32] we used genetic engineering to produce the material components that confer the desired biological functions, namely enzymatic degradability and cell adhesion. In contrast to chemical peptide synthesis, the high fidelity of this production method in terms of molecular size control and amino acid sequence potentially allows the versatile synthesis of larger and highly specialized proteins, which could also bear complex secondary structures such as α-helixes or β-sheets, for a wide range of applications.[33−42] As shown previously,[32] the polypeptides chosen for this study can be cross-linked to form elastic hydrogels via Michael-type conjugate addition, a mild and highly self-selective chemical reaction of cysteine thiols to vinyl sulfone moieties of end-functionalized PEG. This reaction also has the desired advantage of permitting the transformation of the bioactive synthetic matrix from the liquid to the solid state in the presence of living tissue.[43,44] Moreover, the material's structural properties can be optimized by varying gelation conditions such as precursor concentration and stoichiometry of reacting groups.

In the present study, we investigate the hypothesis that specific biological characteristics can be conferred to the matrixes through the design of recombinant protein polymers, as it was previously shown in similar PEG-based hydrogels containing chemically synthesized peptides.[26,27,30,31] We first present a systematic overview of the material's biological functions in vitro ranging from enzymatic degradation characteristics to cell adhesion behavior and three-dimensional cell migration. We then document the in vivo performance of our biomaterials in a model system, where hydrogels served as a provisional matrix and carrier of bone morphogenetic protein (rhBMP-2) for successful bone regeneration in a critical-sized defect of the rat calvarium.

Materials and Methods

Functionalization of Poly(ethylene glycol) with Terminal Vinyl Sulfone Groups. The modification of PEG (Fluka, Switzerland, M_n 6000) to PEG-divinyl sulfone (PEG-di-VS) was previously described.[32] Briefly, after drying PEG by azeotropic distillation with toluene, the functionalization reaction was performed for 6 d at room temperature and under argon in dichloromethane by adding excess sodium hydride (Aldrich, USA) and excess divinyl sulfone in molar ratios with PEG of 1:10 and 1:100, respectively. After the mixture was filtered, the product was precipitated twice in ice-cold diethyl ether and recovered by filtration. The precipitate was extensively washed with diethyl ether and dried in vacuo. A total of 95% ± 2% end group conversion was calculated based on NMR analysis.

Protein Polymer Expression. As previously described,[32] the genes encoding the monomers of two biofunctional polypeptides (protein polymers) differing in their sensitivity to proteases were created de novo by recursive PCR using overlapping single-stranded DNA fragments as templates.[45] These monomers were subsequently multimerized using nonpalindromic restriction sites (BstDS I) as linkers. The multimers of interest (Table 1) were then cloned into the expression vector pET 14b (Novagen), each containing a thrombin-cleavable polyhistidine-tag (His-tag) at its N-terminus for Ni^{2+}-affinity purification. The protein polymers were expressed in batch cultures of *Escherichia coli* and purified using Ni^{2+}-affinity chromatography. Intra- and intermolecular disulfide bonds (−S−S−) were reduced with tris-(2-carboxyethyl)phosphine hydrochloride (TCEP·HCl, Pierce, USA) and dialyzed in degassed double deionized water (ddH_2O) under argon, followed by lyophilization. Mass spectroscopy and amino acid analysis (total amino acid content and N-terminal sequencing) confirmed protein identity, while Ellman's test for the detection of free thiols was used to prove complete reduction of protein thiols (Table 1).

Hydrogel Formation. Hydrogels were prepared via Michael-type conjugate addition of the protein polymer thiols (Table 1) to vinyl sulfones of end-functionalized PEG (PEG-di-VS, M_n 6000). Protein polymers and PEG-di-VS were resuspended separately in 0.45 M triethanolamine buffer (TEA buffer, Aldrich, USA) at pH 7.7 at desired concentrations. For example, to make 50 μL of stoichiometrically

balanced (r = SH/VS = 1) hydrogels at 9.5% w/v, 2.01 mg of degradable dimeric protein polymer was dissolved in 30 μL of TEA and mixed with 20 μL of a 0.128 mg/μL PEG-di-VS solution. After mixing, the solution was pipetted onto a sterile hydrophobic glass microscope slide (coated with SigmaCote; Sigma) with 1 mm thick spacers at both ends. A second hydrophobic glass microscope slide was positioned and clamped with binder clips over the lower slide so that the drop of precursor solution spread to form a disk between the two hydrophobic surfaces. The cross-linking reaction (i.e. gelation) was allowed to proceed for 1 h at 37 °C in a humidified atmosphere. The hydrogels were then stored in buffers of choice for further investigation. For the production of all hydrogels described here, the PEG-di-VS precursor solution was kept at a constant concentration (0.128 mg/μL) whereas the concentration of different protein components was adjusted according to the measured M_w (Table 1) and the desired stoichiometry. Hydrogels prepared at different overall concentrations of 9.5%, 7.5%, and 5.5% (w/v) were formed by diluting concentrated stock solutions (9.5%, w/v) to minimize weighing error. Mass percent and stoichiometric ratio r of the precursors are stated individually in each case and in Table 1.

Biochemical Degradation of Hydrogels. A total of 40 to 50 mg hydrogels (after swelling) obtained from 20 μL of precursor solution at 9.5% w/v (r = 1 for the gels made with both dimer proteins and the tetramer nondegradable, and at r = 1.1 for gels made with the tetramer degradable; Table 1) were incubated at 37 °C in suitable buffers (for plasmin degradation: 20 mM Tris, 150 mM NaCl, pH 7.6; for MMP degradation: 50 mM tricine, 50 mM NaCl, 10 mM $CaCl_2$ and 0.05% brj-35, pH 7.5) with 0.075 U/mL human plasmin (Roche) or 5 nM MMP-1 (kindly provided by Dr. H. Nagase, Imperial College of Science, Technology and Medicine, London). Proteolytic degradation of hydrogels was monitored by measuring the volume change (overall swelling) due to degradation.

In Vitro Cell Experiments. Human foreskin fibroblasts (HFFs; neonatal normal human dermal fibroblast, Clonetics) were cultured under standard cell culture conditions in Dulbecco's Modified Eagle's Medium (DMEM) with 10% heat-inactivated fetal bovine serum (FBS) and 1% antibiotic-antimycotic (Gibco-BRL/Life Technologies AG, Switzerland). Cultures were kept at 37 °C and 5% CO_2. HFFs used in experiments were from passages between 5 and 12.

Cell Adhesion to Hydrogel Surfaces. Characterization of cell adhesion on hydrogel surfaces was performed in serum-free medium. Cells were cultured at a density of 5000 cells/cm^2 for 4 h on synthetic hydrogels prepared from protein polymer dimers and PEG-di-VS (9.5% w/v, r = 1) and, for comparison, on 0.2% w/v fibrin gels. In competitive inhibition studies, serum-free cell culture medium was supplemented with the soluble oligopeptide cyclic-RGDFV (Calbiochem) at concentrations 0, 7, and 35 μM. After 4 h of culture the cells were fixed with 4% formalin, permeabilized with 0.1% Triton X-100, and washed with PBS. Cytoskeletal F-actin fibers and nuclei were stained with rhodamine-labeled phalloidin and DAPI (Molecular Probes Inc.), respectively (for details, see staining section). Images were recorded using a Zeiss Axiovert-135 inverted phase contrast microscope (Zeiss, Oberkochen, Germany).

Three-Dimensional Cell Migration. Cell migration in degradable and nondegradable matrixes was investigated using a 3D cell invasion assay previously described elsewhere.[24] Briefly, HFF-fibrin clusters (ca. 1−2 μL in volume) consisting of 0.2% w/v fibrin and containing 35 000 cells/μL were immersed just prior to cross-linking inside 25 μL of precursor solution to prepare protein-PEG hydrogel disks as described above. Gelation of hydrogel disks containing one or two clusters each occurred in a humidified atmosphere at 37 °C in 1 h. The disks were then transferred into individual wells of a 12-well cell culture plate containing 2 mL of complete cell culture medium per well. Aliquots from identical fibrinogen and thrombin stock solutions were used to make all HFF-fibrin clusters, and large batches of the different precursors for synthetic hydrogels were processed to guarantee reproducibility. Macroscopic material characteristics of cell-free protein-PEG matrixes were monitored, as described previously,[32] for each 3D migration assay by casting identical hydrogel disks without HFF-fibrin clusters.

In the protease inhibition studies, either bovine lung aprotinin (an inhibitor of serine-proteases including plasmin; Calbiochem, USA) or GM6001 (a broad MMP inhibitor; Chemicon, Germany), or the combination of both, were added to the cell culture medium 1 day after starting cell culture with the protein-PEG gels containing HFF-fibrin clusters (day 1). During inhibition studies, the inhibitor concentrations (aprotinin: 50 μg/mL and GM6001: 25 μM) were maintained constant by exchanging the cell culture medium every 2 d at original inhibitor concentrations. On day 6, protease inhibition was terminated by continuing the culture in complete medium without inhibitors. Cell migration from HFF-fibrin clusters into the synthetic protein-PEG matrixes was imaged using inverted phase microscopy (Zeiss Axiovert 135, Zeiss, Switzerland) and quantified in the clusters' center plane using the Leica QWin image analysis software package (n = 4−6).

Staining and Confocal Microscopy. Cells within, and on the surface of, hydrogels were fixed with 4% formalin solution (Sigma) for 1 h or 15 min, respectively, permeabilized with 0.2% Triton X-100 for 15 min, and washed repeatedly with PBS. Cell nuclei were stained with 1 μg/mL 4′,6-diamidino-2-phenylinodole (DAPI; Molecular Probes) for 20 or 10 min, respectively. Cytoskeletal F-actin fibers were stained for 3 h or 30 min, respectively, with 0.4 units/mL rhodamine-labeled phalloidin (Molecular Probes Inc.) in PBS containing 1% serum albumin. After staining, the samples were washed with PBS. Confocal laser scanning microscopy (CLSM) was performed on cells migrating from cell-fibrin clusters into synthetic matrixes using Leica's TCS SP2 system (Leica Microsystems, Bensheim, Germany).

In Vivo Experiments: Bone Healing of Critical-Sized Defects in the Rat Calvarium. Surgery for the creation of defects in the calvarium of adult female Sprague−Dawley albino rats and histological processing of explants was performed as described elsewhere.[27,30,46] Briefly, a calvarial defect with a diameter of 8 mm was created in the parietal bone with a dental handpiece. Preformed hydrogel disks (with corresponding diameter and 1 mm in thickness) were placed into the defect after careful removal of the calvarial disk while avoiding dural perforation, and after rinsing the surgical site with saline to remove bone debris. After five weeks, rats were sacrificed, explanted sculls were radiographed, and cross-sections of the defects were prepared for histology by staining with toluidine blue O and Goldner Trichrome (Sigma, Buchs, Switzerland). Micro-computed tomography and three-dimensional image analysis were performed as described by Lutolf et al.[27] using a μCT 40 imaging system (Scanco Medical, Bassersdorf, Switzerland), and included the measurement of the following parameters characterizing bone formation in the defect region: *Bone volume* defined as total volume of bone formed; *bone connectivity density* expressing the density of bone connections within the bone volume; and *bone coverage* calculated from a projection of the cranium in superior−inferior direction to create a high-resolution radiograph-like images.

Critical-sized defects were filled with matrixes of degradable and nondegradable protein polymer dimers (9.5% w/v; r = 1), both gelled with PEG-di-VS and with a content of 5 μg of rhBMP-2 per gel. rhBMP-2, prepared as described elsewhere,[47] was physically entrapped in the matrixes by mixing the growth factor with the PEG-di-VS precursor solution prior to gelation. After gelation (1 h at 37 °C), individual disk-shaped hydrogels were stored in PBS at 4 °C. Controls consisted of matrixes without rhBMP-2. (n = 5−7).

Results and Discussion

A. Mimicking the Natural Extracellular Matrix. *Degradation of Hydrogels Depends on the Proteolytic Degradability of the Protein Polymer Backbone.* We previously reported the biochemical properties of protein polymers in soluble form, utilized herein for cross-linking with PEG-di-VS.[32] We dem-

Chart 1. (A) Proteolytically Degradable and Nondegradable Recombinant Protein Polymer Constructs,[a] and (B) Schematic of Hydrogel Formation and Cross-Linking Reaction[b]

A

Degradable construct:

MGSSHHHHHHSSGLVP**R**↕GSHMEEGG**C**(HGGL**R**GDFSSANNR↓DNTYEEGG**C**GGEEGPQG↑IAGQ**R**GVIDS**C**)$_n$ HGGEEG
(n = 2 and 4) Fibrinogen fragment Collagen fragment

Non-degradable construct:

MGSSHHHHHHSSGLVP**R**↕GSHMEEGG**C**(HGGL**R**GDFSSANN***G***DNTYEEGG**C**GGEEG***D***QGIAG***FP***G***S***IDS**C**)$_n$ HGGEEG
(n = 2 and 4)

B

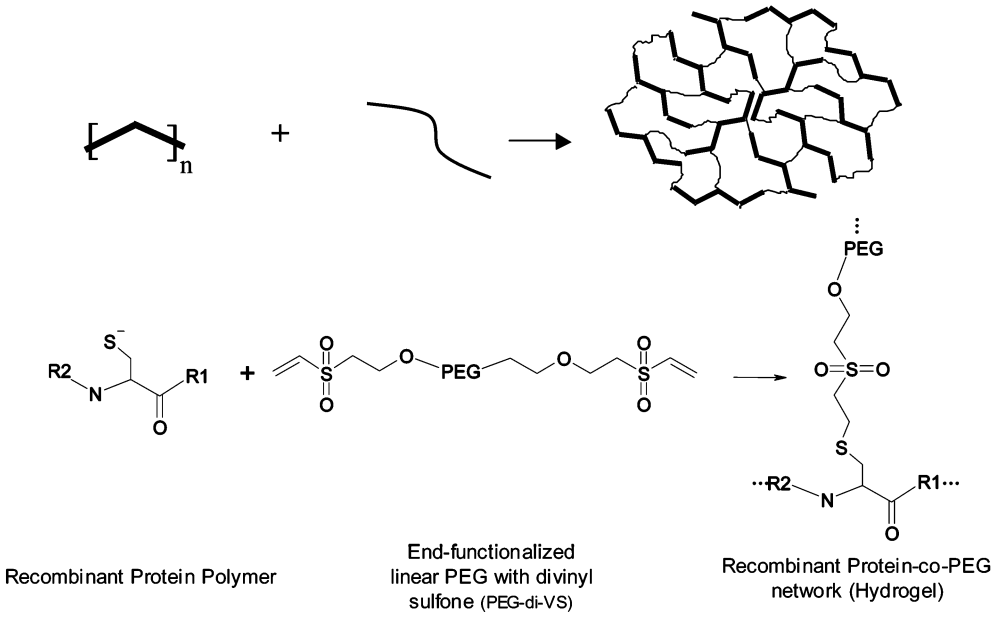

[a] One letter amino acid code: alanine (A), arginine (R), asparagine (N), aspartic acid (D), cysteine (C), glutamic acid (E), glutamine (Q), glycine (G), histidine (H), isoleucine (I), leucine (L), lysine (K), methionine (M), phenylalanine (F), proline (P), serine (S), threonine (T), tryptophan (W), tyrosine (Y), valine (V). (↓) Designed cleavage site for plasmin. (↑) Designed cleavage site for matrix metalloproteinase (MMP). (vertical tautomer) Thrombin-cleavable site for removal of His-tag used for recombinant protein purification throughout nickel-affinity chromatography. (**R**) Additional potential plasmin degradation positions found experimentally C-terminally to the indicated arginine (described by Rizzi and Hubbell[32]). Substituted amino acids to rend both designed cleavage sites (plasmin and MMP) nondegradable are italic and bold. Thiol residues of cysteine amino acids (C) represent designed cross-linking sites for hydrogel formation. [b]Adapted from Rizzi and Hubbell.[32]

onstrated the successful biosynthesis of engineered protein polymers containing specific MMP- and plasmin-degradable sites as confirmed by N-terminal sequencing of degradation products after incubation with MMP-1 and plasmin (Chart 1). Protease degradation sites were rendered inactive by amino acid substitution. However, unexpected plasmin degradation sites at C-terminal arginine residues (Chart 1) were also identified in both degradable and presumed nondegradable protein constructs. In particular, the RGD cell-adhesion site was found to be cleavable by plasmin C-terminally to the arginine residue under experimental conditions.

To investigate degradation of our protein-PEG hydrogels by proteolysis, we employed the volume-change method as previously utilized by Lutolf et al. for similar hydrogel systems.[30] The degradation characteristics of hydrogels (Figure 1) correlated directly with the properties of each hydrogel's protein polymer constituent in soluble form.[32] For instance, hydrogels formed from degradable protein constructs and incubated with MMP-1 or plasmin started to swell due to bulk enzymatic degradation until collapsing,[30] (Figure 1A,B). In contrast, no degradation was observed using this method in the case of hydrogels formed from nondegradable protein constructs that were exposed to MMP-1. Nondegradable gels remained unaffected by MMP-1 as manifest in constant gel volumes during incubation with protease (Figure 1A). However, slow swelling of presumed nondegradable matrixes was measurable in response to plasmin, in agreement with the finding that unexpected sites in the protein polymers were susceptible to slow degradation by plasmin, namely the RGD cell-adhesion site present in all constructs. As illustrated in Figure 1B, the degradation rate of nondegradable matrixes during plasmin exposure was significantly slower compared to that of degradable matrixes. Furthermore, the swelling rate of nondegradable hydrogels tended to slow during plasmin incubation. This was probably due to loss of enzyme activity after long incubation periods (presumably caused by autoproteolysis of enzyme). Ultimately, nondegradable hydrogels remained intact for several weeks (data not shown).

Upon exposure to proteases, the observed volume increase of the degradable hydrogels (Figure 1) indicates a predominance of bulk over surface degradation of the network.[30,48] This implies that proteases reached homogeneous distribution within the hydrogels in the course of network degradation. According to Lutolf et al., in the case of the MMP-1 degradation studies (Figure 1A), the concentrations of the protease (5 nM) and of the corresponding GPQG↓IAGQ-substrate (2.43 mM and 3.63 mM for the degradable dimer and tetramer, respectively) were

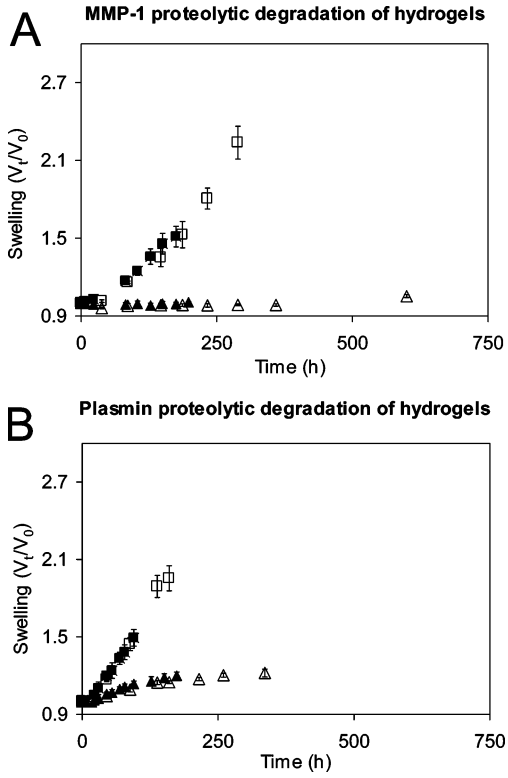

Figure 1. Proteolytic degradation of hydrogels. Swelling defined as the ratio V_t/V_0, where V_t is the total volume at time t during proteolytic degradation and V_0 is the initial volume of gel prior protease incubation, was utilized to monitor hydrogel response to incubation in MMP-1 (A) and plasmin (B). Gel networks formed by cross-linkers containing designed protease substrates (■ for dimer and □ for tetramer protein construct, in A and B) showed a rapid increase of swelling upon gel dissolution, indicating bulk degradation of networks. By contrast, hydrogels formed with the nondegradable protein constructs either remained stable while incubated in MMP-1 (▲ for dimer and △ for tetramer in A) or slightly swelled over the investigated period in plasmin (▲ and △ in B) but did not fall apart over weeks (data not shown). Average of $n = 4$ per point; bars correspond to standard deviation.

within a range to result in a zero-order rate of hydrolysis, i.e. with the enzyme being fully saturated with substrate[30]

Taken together, these findings show conclusively that the sensitivity of hybrid-hydrogels to specific proteolytic degradation can be controlled through the rational design of chemically and genetically engineered biological components.

Hydrogels Promote Cell Adhesion. The fibrin-derived RGD site incorporated in our protein constructs, which was intended to produce the cell-binding properties of our protein polymers (Chart 1), was also used by Halstenberg et al. to effect cell adhesion to a similar recombinant protein polymer.[24] An increase in cell adhesion to coated tissue-culture polystyrene (TCPS) was observed when increasing the concentration of adsorbed protein polymers on the surface. Cell adhesion was inhibited by increasing the medium concentration of a soluble competing integrin ligand, namely the cyclic RGD-peptide, cyclic-RGDFV. Moreover, the protein polymer containing the mutated RGD site, namely RGG, did not support cell adhesion, indicating the specificity of cellular interaction—via integrin receptors—with the RGD site that was present in the protein polymers.[24] In agreement with these findings, Figure 2 illustrates cell adhesion to 0.2% fibrin gels (Figure 2A) versus cell adhesion to the investigated synthetic matrixes (Figure 2B). Generally, HFFs adhered and spread similarly on fibrin gels and synthetic matrixes, both after 4 h of culture in serum-free medium (Figure 2A,B). The specificity of cell binding to the RGD-site present in these synthetic matrixes was tested by addition of soluble cyclic-RGDFV peptide to the cell culture medium. Competitive inhibition with the cyclic-RGDFV peptide was used here as a negative control for RGD-based cell adhesion in lieu of a nonadhesive protein construct such as one in which the RGD sites could have been mutated or otherwise rendered inactive. Consistent with many examples in the literature,[24,49−56] soluble cell adhesion ligand cyclic-RGD competitively inhibited cell spreading on our synthetic hydrogels in a concentration dependent manner (Figure 2B−D). This finding indicates that the RGD site present in our matrixes is specifically active in promoting cell adhesion and spreading.

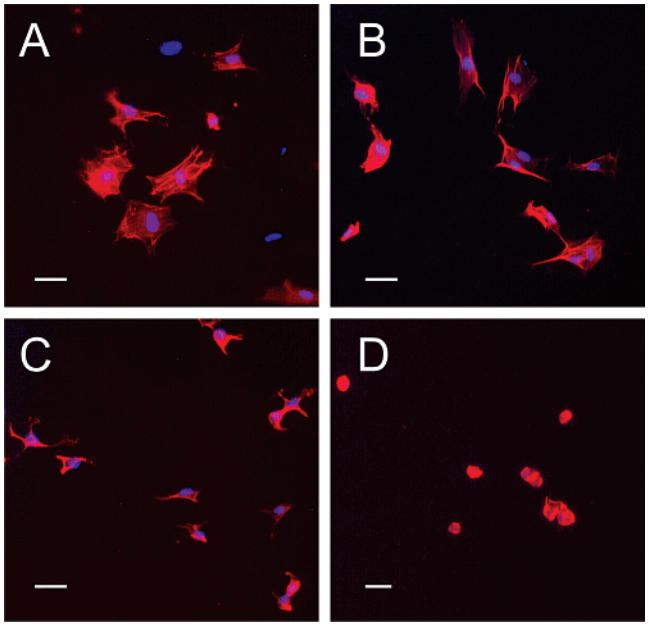

Figure 2. Cells cultured for 4 h in serum-free medium on 0.2% fibrin gels (A); and on protein-PEG matrixes in the presence of 0 μM (B), 7 μM (C), and 35 μM (D) soluble cyclic-RGDFV peptide and subsequently stained for nuclei (with DAPI, blue) and actin filaments (Rodamine-labeled Phalloidin, red). Scale bars correspond to 50 μm.

B. Matrix Components and Physical Characteristics Influence Cell Migration. Specific features of natural matrixes, including sensitivity to enzymatic degradation and the ability to promote cellular adhesion, were successfully conferred to synthetic polymer networks. Cell adhesion represents, among other factors, a prerequisite for cell movement on two-dimensional (2D) surfaces.[57,58] In contrast, cells migrating across 3D matrixes additionally have to deal with the physical obstruction posed by the matrix itself.[22,59] In nature, to overcome this impediment, the cells generally remodel their immediate environment proteolytically[18,22] and/or pursue preexisting holes by adapting their cellular morphology.[22,60] In our work, using materials that lack preexisting cell-sized pores, we focus on the importance of cell-mediated proteolysis and on the influence of mechanical properties on cell migration within protein-PEG matrixes.

Cell Migration into Proteolytically Degradable Matrixes. As illustrated in Figure 3A, we observed radial invasion of cells from HFF-fibrin clusters into proteolytically degradable protein-PEG matrixes that were made from degradable protein dimer and PEG-di-VS at $r = r_{opt} = 1$ and 9.5% (w/v) (Table 1). In general, cells migrating within 3D matrixes assumed a spindle-like shape in contrast to the spread cells observed on surfaces (Figure 2A,B). Furthermore, HFFs migrating out of cell-fibrin clusters into protein-PEG matrixes maintained intercellular

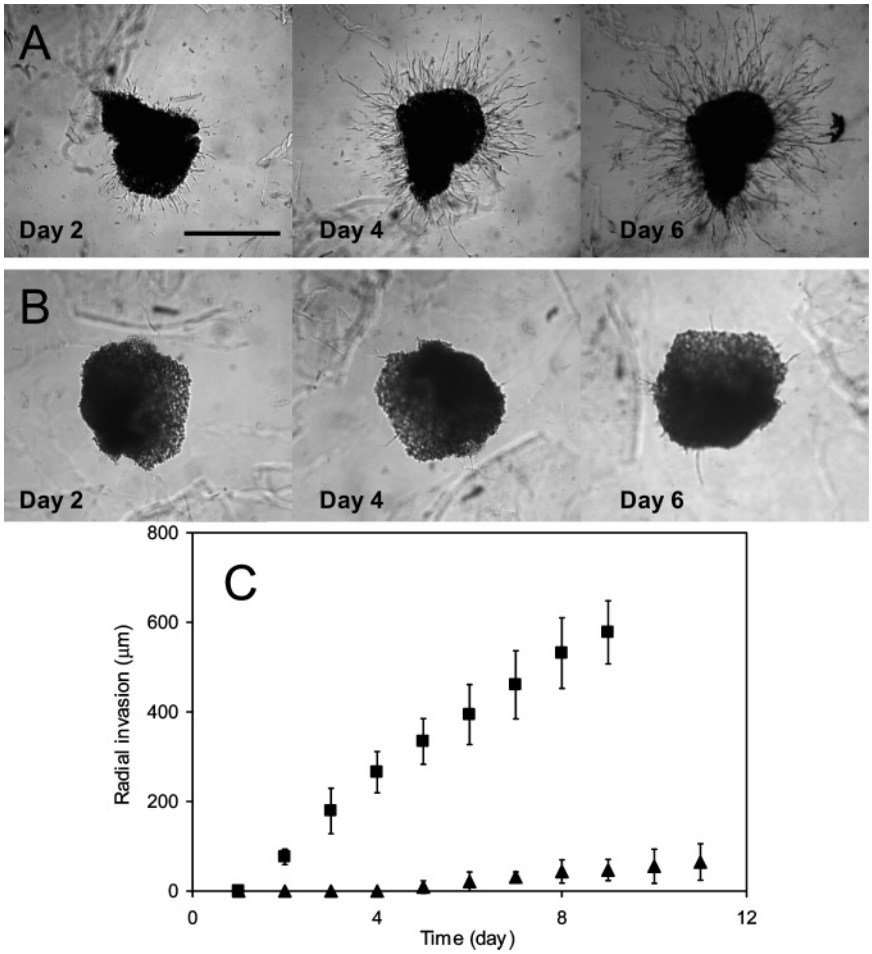

Figure 3. Three-dimensional fibroblast migration in different protein-PEG matrixes. Fibroblast outgrowth in three dimensions from hFF-fibrin clusters into degradable (A) and nondegradable (B) cell-adhesive protein-PEG matrixes (9.5% w/v, $r = 1$; Table 1) formed with the dimer protein constructs (illustration of hFF migration at day 2, 4, 6 in culture; ■ and ▲ in C, respectively). In general, (C) cell invasion distance increased approximately linearly with time and was dramatically reduced or absent in matrixes formed with nondegradable protein constructs ($n = 5-6$, error bars correspond to SD). Noteworthy, proteolytically degradable and nondegradable protein-PEG matrixes displaying similar structural properties and density of cell-binding sites (RGD) showed significantly different cellular invasions, indicating that matrix sensitivity to proteolysis was the main factor influencing the outgrowth of cells. Bar corresponds to 500 μm (B).

contact as visualized by confocal laser microscopy of cells double-stained for nuclei and actin filament (Figure 5H). A similar type of cell migration, namely cohort cell migration,[61] was previously reported by Halstenberg et al.,[24] Lutolf et al.,[30] and Pratt et al.[31] using identical cell invasion assays. HFF migration started on day 2 ± 1 after HFF-fibrin clusters were embedded in synthetic matrixes (Figure 3A). Thereafter, the migration distance away from the clusters was approximately linear with culture time (Figure 3C). A similar time-dependence of cell outgrowth was previously observed only for synthetic matrixes that were entirely enzymatically degradable.[30] In matrixes that degraded by cell-associated enzymatic activity and bulk hydrolysis simultaneously, cell migration ceased within a few days due to rapid loosening of matrix caused by bulk hydrolysis.[24] In contrast, the matrixes presented here, which were designed to be degradable only by proteolysis, remained intact and stable, maintaining their mechanical integrity up to one month in cell culture. The long-term stability of hydrogels in cell culture as well as the sustained cellular outgrowth over time are evidence for cell-associated proteolysis localized exclusively at the cell periphery[7,30] rather than bulk degradation caused by passive hydrolysis or diffusion of proteases.

Matrix Sensitivity to Proteolytic Degradation Affects Cell Invasion of 3D Structures. Matrix sensitivity to proteases and the resulting effect on cell migration were investigated for protein-PEG hydrogels formed from degradable and nondegradable protein dimers (9.5% w/v, $r = 1$, Table 1). As previously reported,[32] both hydrogel systems displayed similar network properties (Table 1). These matrixes exhibited distinct degradation profiles upon protease exposure (Figure 1), and the rate of cell migration corresponded to these differences as illustrated in Figure 3: cells hardly migrated at all in networks consisting of the nondegradable protein dimer, and the number and density of radial cell outgrowths were very small compared to those in degradable matrixes.

Cell Migration into Proteolytically Degradable Protein-PEG Matrixes Depends on MMP Activity. To verify that proteolytic degradation is necessary and accounts for the differences in HFF migration, protease inhibition studies were performed. Interestingly, these investigations revealed that HFF migration in the degradable protein-PEG networks (formed with dimer degradable, 9.5% w/v, $r = 1$; Table 1), containing both plasmin and MMP sensitive sites, depended primarily on MMP activity (Figure 4). Addition of a broad-spectrum MMP inhibitor (GM6001, 25 μM) completely stopped cell invasion of 9.5% (w/v) degradable matrixes (Figure 4). After discontinuing MMP inhibition on day 6, cells started to invade the surrounding matrixes (Figure 4C,D; day 12) and outgrowth continued just like in un-inhibited cultures without prior protease inhibition. However, with protease inhibition, a lower density of outgrowths

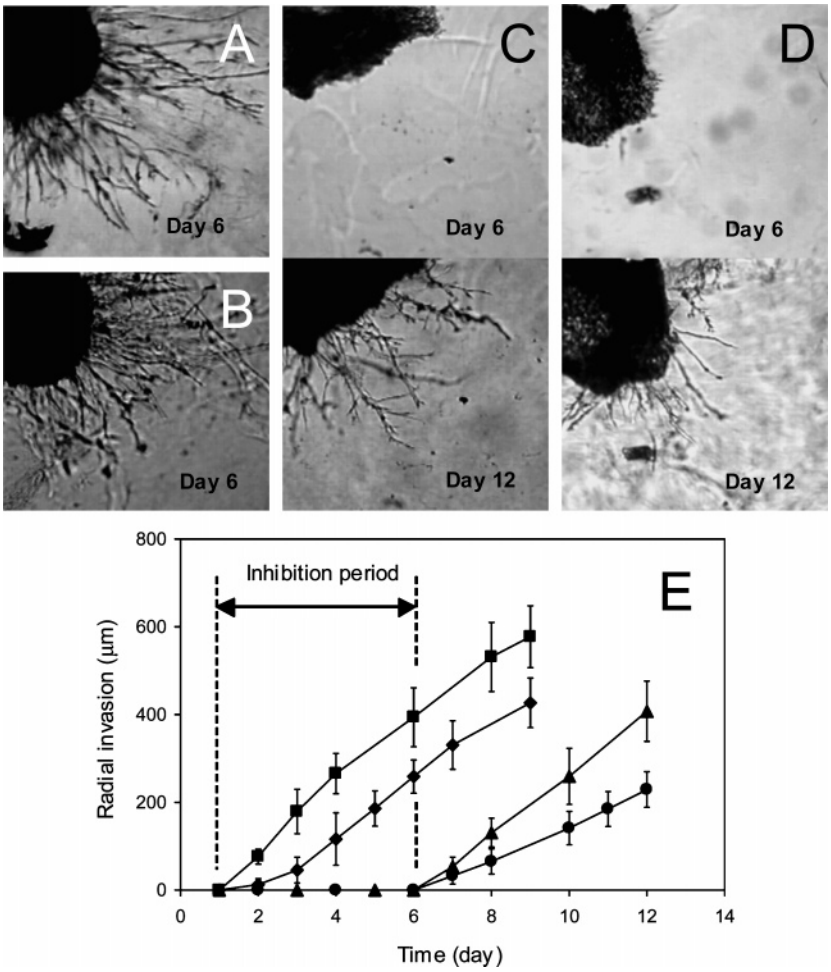

Figure 4. Inhibition of fibroblast migration into protein-PEG matrixes prepared with dimer degradable protein construct and PEG6000-di-VS (9.5% w/v, $r = r_{opt}$; Table 1). Cell outgrowth from hFF-fibrin clusters into degradable protein-PEG matrixes in the absence of any inhibitor (A at day 6; ■ in E). In the presence of 50 μg/mL aprotinin (B, at inhibition end: day 6; ◆ in E) cell migration was normally retarded by 1 to 2 d, but its rate remained approximately similar to noninhibited conditions. In contrast, migration was totally inhibited either in the presence of 25 μM GM6001 alone or in combination with 50 μg/mL aprotinin (C and D upper, respectively, at inhibition end = day 6; ▲ or ● in E, respectively). After stopping both inhibition conditions with GM6001 alone and in combination with aprotinin at day 6, HFFs started to migrate from hFF-fibrin clusters into matrixes (C and D lower, respectively, 6 days after inhibition end = day 12) in a similar manner as observed in noninhibited samples (A). However, the density of outgrowths was lower than in noninhibited samples. (E) Three-dimensional HFF outgrowth from cell-fibrin clusters into degradable protein-PEG matrixes at different inhibition conditions. The inhibition period lasted from day 1 to day 6, indicating that at present conditions the cell-driven MMP degradation system played a key role for cell migration into proteolytically degradable protein-PEG matrixes. (In E: average of $n = 4-6$ per point; error bars correspond to SD).

resulted, in all probability because of reduced cell viability after 6 d of cell confinement due to protease inhibition. In contrast, the effect of aprotinin, a serine-protease inhibitor (50 μg/mL), was less dramatic (Figure 4B,E). Most notably, the presence of aprotinin in the cell culture medium merely tended to delay the start of cell outgrowth from HFF-fibrin clusters by 1 to 2 days (Figure 4E) and reduced the density of cellular outgrowths (Figure 4B). Subsequently, however, outgrowth continued with a similar rate as observed in the absence of any protease inhibition (Figure 4E). A recently published study by our group reports that single cell (HFF) migration within exclusively plasmin-sensitive PEG gels was mostly suppressed, suggesting that the plasmin(ogen) system in HFF was lacking of one or more components.[59] In our study, cells reside first within a fibrin matrix. Fibrinogen typically contains traces of plasminogen,[21,62,63] which can be activated by cells to form plasmin by which the fibrin matrix is rapidly degraded.[21,62,64] Hence, we believe that HFFs can emerge from their original fibrin matrix and move on into the synthetic hydrogel surrounding them via cell-activated plasmin. The delay in the onset of cell migration under conditions of serine protease inhibition by aprotinin was probably due to the cells' compromised ability to penetrate and migrate out of the fibrin clusters in which they reside at first. As a consequence of inhibition by aprotinin, the cells probably had to switch to alternative strategies to overcome the fibrin barrier, such as fibrinolysis by MMPs[65 66] and/or mechanical rearrangement of the fibrin matrix.[67]

These protease inhibition studies raised the question whether plasmin- or MMP-mediated matrix degradation was the dominant mode of cell penetration into protein-PEG matrixes. Studies conducted by Hiraoka et al.[65] and Hortary et al.[66] have revealed the presence of an alternative proteolytic mechanism besides the plasmin(ogen) system involving membrane-anchored MMPs for cell invasion within fibrin matrixes. Moreover, Lung et al. reported functional overlap between the two classes of matrix-degrading proteases in vivo during wound healing in fibrin-rich provisional matrixes.[8] These findings underscore the importance that the MMPs system could have in the proteolytic remodeling of our protein-PEG matrixes. Alternatively, fibrin can provide the missing component(s) of the plasmin(ogen) system (e.g. plasminogen)[21,62,63] and enable HFF migration within plasmin-sensitive PEG matrixes as previously observed

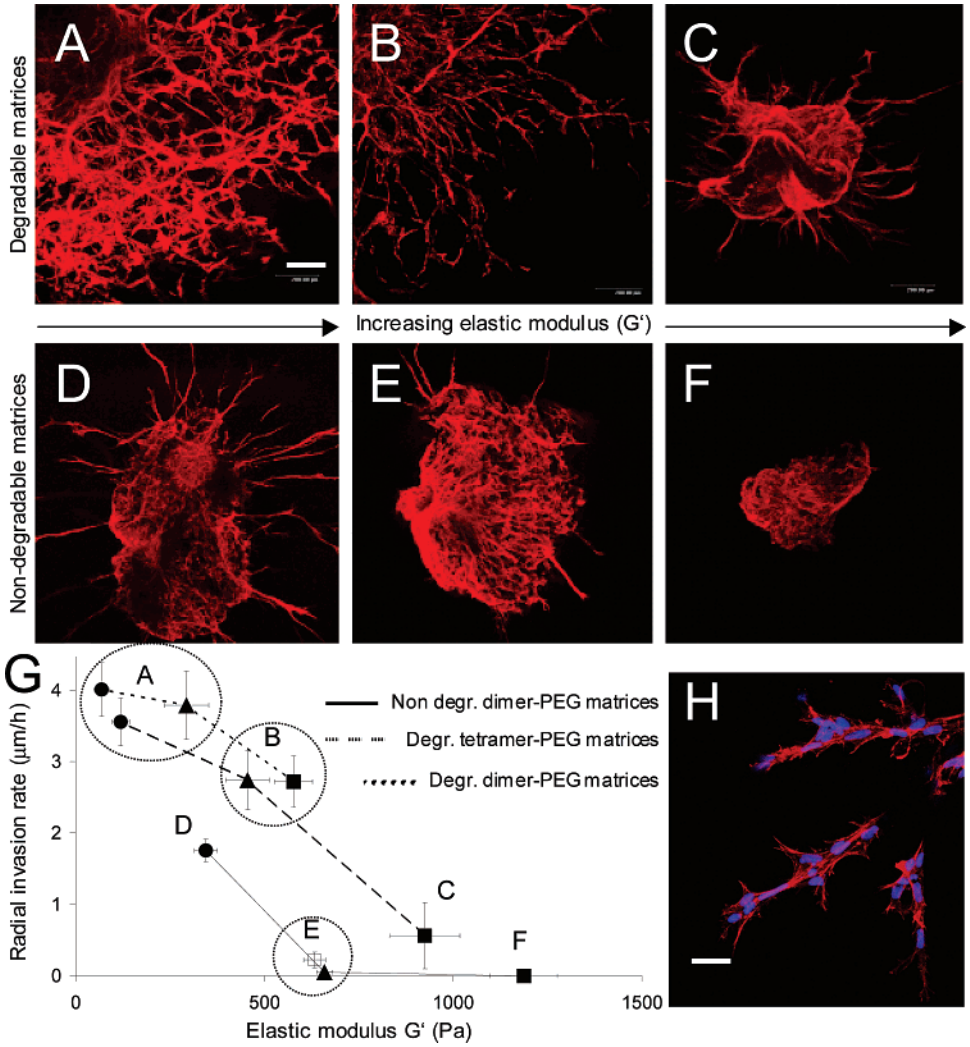

Figure 5. Influence of the matrix mechanical properties on density and migration rate of invading cells. CSLM images showing typical spindle-like shaped fibroblasts migrating in a cohort manner from cell-fibrin clusters into degradable (A−C; H at higher magnification), or nondegradable (D and F) protein-PEG matrixes on days 12 (for C) and 14 (for the rest). (G) HFF invasion rates were plotted against the mechanical properties of the matrixes at different compositions: ● for 5.5%, ▲ for 7.5%, ■ for 9.5% (w/v) matrixes at r_{opt}; and □ for the 9.5% (w/v) gels at $r = 1$ formed with the nondegradable dimer (Table 1). Both migration distance and density of invading cells decreased with increasing elastic moduli from weak (G' <300Pa; A) to harder (G' >500Pa; B and C) degradable gels. In the nondegradable matrixes, migration distance and density of invading cells were dramatically reduced (G' <300Pa; D) or even absent (G' >600Pa; E and F). Bar corresponds to 200 μm in A−F and to 40 μm in H. Blue corresponds to cell nuclei and red corresponds to actin filaments, stained with DAPI and rhodamine-labeled phalloidin, respectively.

by Halstenberg et al.[24]and Pratt et al.[31] employing a similar migration assay as here. According to Halstenberg et al., HFF migration in plasmin sensitive protein-PEG matrixes was almost totally inhibited by addition of aprotinin, a plasmin inhibitor, at a concentration of 50 μg/mL.[24] In our hydrogel system, similar aprotinin concentrations were not so effective, probably because cells also relied on MMP degradation sites to invade the synthetic matrixes. Accordingly, there was no difference in cellular migration between MMP inhibition alone or in combination with plasmin inhibition by aprotinin (Figure 4), implying again that plasmin-mediated degradation did not play a relevant role in our hydrogel system. Although degradable protein-PEG matrixes were degraded by plasmin in our biochemical experiments (Figure 1), significantly lower concentrations of active plasmin in cell culture may explain its secondary role in promoting proteolytically mediated cell migration as shown in these inhibition studies. Consequently, substrates with higher sensitivity to plasmin degradation and/or the addition of exogenous components of the plasmin(ogen) system are presumably required to observe cell migration driven by plasmin proteolysis in these protein-PEG matrixes, as previously reported by Pratt et al.[31] In conclusion, HFF migration across degradable protein-PEG matrixes that contained both plasmin and MMP sensitive sites was enabled primarily by MMP activity as confirmed by the negative control, namely inhibition with the broad spectrum MMP inhibitor GM6001.

However, additional studies on the expression−activation profiles of the protease systems, plasmin(ogen) and MMPs, by the HFFs and on cleavage kinetics of the corresponding substrates designed within the protein polymers, may be helpful to elucidate the role of the different proteolytic pathways in this cell migration assay.

Physical Properties of Protein-PEG Matrixes May Affect 3D Cell Migration. In general, within each matrix system, the rate of cell invasion (Figure 5G), the density of cellular outgrowths, and the interconnectivity of migrating cells, as recorded by confocal scanning laser microscopy (Figure 5A−C for the degradable and Figure 5D−F for the nondegradable hydrogels), became less with increasing elastic modulus. However, as the bulk mechanical properties of the different matrixes were a function of overall precursor concentration at fixed stoichiometric ratio $r = r_{opt}$, in these protein-PEG hydrogels it was not

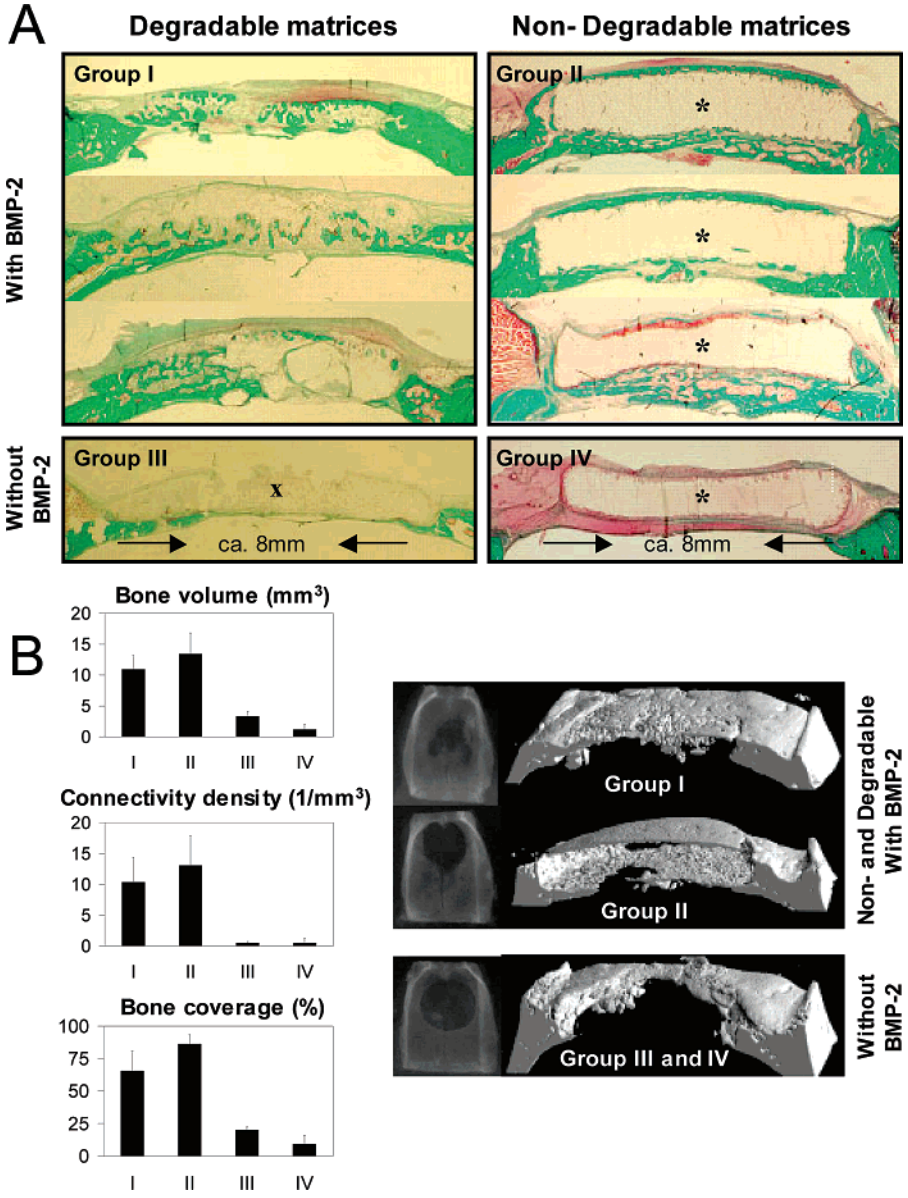

Figure 6. Healing of critical-sized defects in rat calvaria after 5 week implantation. (A) Selection of representative histological sections after treatment of rat calvarial defects at various conditions. Proteolytically degradable hydrogels containing 5 μg of rhBMP-2 were completely or partially replaced by calcified bone, stained in green with Goldner Trichrome (Group I, selection from three different animals). In contrast, nondegradable matrixes carrying rhBMP-2 remained almost intact after 5 week implantation (hydrogel marked with $*$) and newly formed bone was, normally, found at matrix margin (Group II, selection from three different animals). No bone formation was observed in rat calvarial defects treated with control samples without rhBMP-2 (Groups III and IV). Proteolytic degradable matrixes were infiltrated and almost completely remodeled by fibroblast-like cells (Group III, area marked with x), whereas nondegradable hydrogels stayed intact over the implantation period (Group IV). (B) Quantitative evaluation of bone formation in the rat calvarial defects (left panel) after the different treatment conditions, and the corresponding radiographic (middle) and three-dimensional microcomputed tomography images (right panel). Histograms (left panel) illustrate results from microcomputed tomography analysis displaying parameters characterizing bone formation in the defect region. These data confirmed the key role of BMP-2 in inducing bone formation (histograms). No difference was observed in the amount of bone formed when defects were treated with degradable (Group I) and nondegradable (Group II) matrixes in the presence of rhBMP-2. However, in Group I bone was prevalently observed to have replaced the matrix, whereas in Group II bone was confined at matrix surface (three-dimensional microcomputed tomography images and histology sections in A). $n = 7$ for Group I and $n = 5$ for Group II to IV; error bars represent SD.

possible to independently alter physicochemical characteristics and cell-adhesion site density (Table 1). Consequently, the influence of the latter on cell migration could not be investigated separately. Indeed, cell invasion rate was previously reported to depend on cell ligand density.[25,30] The biphasic behavior of the migration rate as a function of cell adhesion-site density reported by Lutolf et al. presumably suggests a less pronounced influence at higher cell adhesion-site concentrations possibly due to saturation of the corresponding cell-surface receptor.[30] As the density of cell-binding sites in our protein-PEG matrixes ranged between 1.41 and 3.63 mM (Table 1), i.e. approximately 5 to 10-fold higher than the greatest concentration reported by Lutolf et al. (350 μM), we mainly attribute the differences in cell migration rates within individual hydrogel systems to their physicochemical properties, rather than to the cell-binding site density (Figure 5G). In contrast to cell migration on 2D substrates, cell movement within densely cross-linked, 3D networks is mostly influenced by the physical obstruction of cells by the matrix.[59] In agreement to previously reported data on synthetic, cell-invadable hydrogels,[30] as the cross-link density in the matrix increased, here reflected indirectly by increasing elastic modulus, the cell migration rate slowed (Figure 5). With

decreasing cross-link density and, thus, decreasing G', cell migration speed increased.

These studies conclusively indicated that mechanical properties of each group of hydrogels may influence cell mobility within 3D matrixes.

Although we strongly believe that cell-associated matrix degradation was the relevant mechanism enabling cell migration as opposed to alternative modes of 3D cell migration proposed by Wolf et al.,[60] we cannot exclude that, at very low mechanical properties, migration through matrix defects may have occurred in our system. For example, at low G', cell invasion (Figure 5D) of nondegradable matrixes seemed to take place along preexisting defects rather than through pathways created by cell-associated proteolytic remodeling of the matrix. Alternatively, other cleavable sites present in all constructs or proteases not tested here could be partially responsible for cell migration in nondegradable matrixes at low cross-linking densities. Lutolf et al.[30] also considered these migration alternatives in their purely synthetic, cell-adhesive, and enzymatically degradable materials upon observing nonnegligible cell invasion despite protease inhibition.

C. Proteolytically Sensitive Matrixes Support Bone Healing. To investigate the role of cell-associated matrix degradation in vivo, hydrogels containing rhBMP-2 were implanted into critical-sized defects in rat calvaria to promote bone regeneration and closure of the defects. Previous studies performed by our groups demonstrated that bone formation induced by rhBMP-2 released from similarly cross-linked PEG-matrixes or collagen sponges was the same,[27] suggesting that BMP-2 activity was not affected during incorporation into synthetic hydrogels.[27,31] Due to its low solubility at physiological pH [68] and the presence of PEG, rhBMP-2 precipitated and was physically entrapped within the network of the PEG-based hydrogels.[27] In these synthetic matrixes rhBMP-2 was shown to be released mainly upon matrix dissolution.[27] However, observations in fibrin matrixes also suggested the possibility that precipitated rhBMP-2 may slowly solubilize in situ and diffuse out of the matrixes.[68] Consistent with previous findings, BMP-2 precipitated at physiological pH, when added to the PEG precursor solution.[27] Due to the strong preference in chemical reactivity of the vinyl sulfone groups of PEG toward free thiols (which should be absent in BMP-2)[69] relative to primary amines as on lysine side chain at physiological pH,[70] we expect the majority of rhBMP-2 to remain noncovalently entrapped in the protein-PEG hydrogels during cross-linking.[27] In agreement with our biological characterization of protein-PEG hydrogels in vitro, cellular infiltration in vivo depended strongly on the degradation properties of the matrixes (Figure 6). Proteolytically degradable hydrogels were infiltrated by cells and were partially or completely resorbed after 5 weeks (Figure 6A, Group I and III), whereas nondegradable matrixes having similar physicochemical properties remained largely intact for at least 5 weeks after implantation into the calvarial defects (Figure 6A, Groups II and IV). Degradable matrixes carrying rhBMP-2 induced intramembranous bone formation as reflected by green staining for calcified bone (Goldner Trichrome staining) within the partially remodeled synthetic matrix (Figure 6, Group I). Interestingly, the results of microcomputed tomography evaluation, represented as bone volume, connectivity density, and coverage in the form of histograms in Figure 6B, did not reflect significant differences in bone formation between defects treated with degradable (Group I) and nondegradable (Group II) matrixes containing rhBMP-2. However, similarly to Pratt et al.,[31] histological sections (Figure 6A) as well as three-dimensional microcomputed tomography images (Figure 6B) of the defects treated with nondegradable hydrogels carrying rhBMP-2 clearly reveal that bone formation was mostly confined to an area at and just outside the tissue−matrix interface (Group II). This finding implies that bone formation was probably induced by the slow release of precipitated rhBMP-2 in the periphery of the implant, rather than by cellular infiltration and bone formation within the implant itself. This observation also suggests that in situ solubilization of rhBMP-2 precipitated within the matrixes, and subsequent release may likely occur also in protein-PEG gels, as previously observed in fibrin matrixes.[68]

Similar successes in healing critical-sized defects of rat calvaria have been reported by Lutolf et al.[27,30] and Pratt et al.[31] using synthetic matrixes formed by PEG macromers cross-linked with small peptides displaying different degrees of sensitivity to proteolytic degradation. Both their and our bioactive hydrogels performed quite similarly in vivo to naturally derived wound-healing matrixes such as collagen,[27] underscoring the potential and importance that more versatile synthetic biomaterials will have in the future.

Conclusions

Biological functions were successfully conferred to artificial ECM analogues as demonstrated in vitro and in vivo. In particular, synthetic protein-PEG hydrogels exhibited properties of natural provisional matrixes that are essential during tissue repair, i.e. the ability of promoting cellular adhesion and of being proteolytically remodeled. Using the same recombinant DNA technology, any known functional protein domain can be incorporated in protein-PEG hydrogels, tailoring the resulting matrix toward any intended medical application. This approach is particularly attractive for the design of artificial proteins carrying combinations of more complex domains, such as structural building blocks (e.g. elastin or collagen-like), cell-receptor binding sites (e.g. fibronectin analogues or growth factors), and a wide range of other functional elements occurring in natural proteins.

Our results emphasize the importance of specific bi-directional biological communication between a provisional therapeutic device and the regenerating tissue. In particular, lack of communication in either direction, absence of specific stimuli, e.g. lack of rhBMP-2, or the inability to respond to a given signal, e.g. sensitivity to proteolytic degradation, led either to the failure to form bone or to an impairment of matrix remodeling. Due to their versatility and specific adaptability to a wide range of medical applications, protein-PEG materials emerge as a powerful alternative to naturally derived matrixes as materials for regenerative tissue engineering.

Acknowledgment. We thank Drs. Heike Hall and Matthias Lutolf for scientific advice and constructive discussions as well as Drs. M. Höchli and T. Bächli of the Electron Microscopy Laboratory at the University of Zurich for the opportunity to use the confocal laser-scanning microscopy. We are grateful to P. Raeber for the drawing in the table of contents graphic.

References and Notes

(1) Clark, R. A. F. *Ann. N. Y. Acad. Sci.* **2001**, *936*, 355−367.
(2) Monaco, J. L.; Lawrence, W. T. *Clin. Plast. Surg.* **2003**, *30*, 1−12.
(3) Basbaum, C. B.; Werb, Z. *Curr. Opin. Cell Biol.* **1996**, *8*, 731−738.
(4) Chen, W. T. *Curr. Opin. Cell Biol.* **1992**, *4*, 802−809.
(5) Birkedal-Hansen, H. *Curr. Opin. Cell Biol.* **1995**, *7*, 728−735.
(6) Greiling, D.; Clark, R. A. F. *J. Cell Sci.* **1997**, *110*, 861−870.
(7) Werb, Z. *Cell* **1997**, *91*, 439−442.

(8) Lund, L. R.; Romer, J.; Bugge, T. H.; Nielsen, B. S.; Frandsen, T. L.; Degen, J. L.; Stephens, R. W.; Dano, K. *EMBO J.* **1999**, *18*, 4645−4656.
(9) Hutmacher, D. W.; Vanscheidt, W. *Drugs Today* **2002**, *38*, 113−133.
(10) Hubbell, J. A. *Curr. Opin. Biotechnol.* **1999**, *10*, 123−129.
(11) Griffith, L. G.; Naughton, G. *Science* **2002**, *295*, 1009-+.
(12) Langer, R.; Tirrell, D. A. *Nature* **2004**, *428*, 487−492.
(13) Lutolf, M. P.; Hubbell, J. A. *Nat. Biotechnol.* **2005**, *23*, 47−55.
(14) Ellingsworth, L. R.; Delustro, F.; Brennan, J. E.; Sawamura, S.; McPherson, J. *J. Immunol.* **1986**, *136*, 877−882.
(15) Delustro, F.; Dasch, J.; Keefe, J.; Ellingsworth, L. *Clin. Orthop. Relat. Res.* **1990**, 263−279.
(16) Lauffenburger, D. A.; Horwitz, A. F. *Cell* **1996**, *84*, 359−369.
(17) Howe, A.; Aplin, A. E.; Alahari, S. K.; Juliano, R. L. *Curr. Opin. Cell Biol.* **1998**, *10*, 220−231.
(18) Murphy, G.; Gavrilovic, J. *Curr. Opin. Cell Biol.* **1999**, *11*, 614−621.
(19) Streuli, C. *Curr. Opin. Cell Biol.* **1999**, *11*, 634−640.
(20) Sternlicht, M. D.; Werb, Z. *Annu. Rev. Cell Dev. Biol.* **2001**, *17*, 463−516.
(21) Ronfard, V.; Barrandon, Y. *Proc. Natl. Acad. Sci. U.S.A.* **2001**, *98*, 4504−4509.
(22) Friedl, P.; Brocker, E. B. *Cell. Mol. Life Sci.* **2000**, *57*, 41−64.
(23) West, J. L.; Hubbell, J. A. *Macromolecules* **1999**, *32*, 241−244.
(24) Halstenberg, S.; Panitch, A.; Rizzi, S.; Hall, H.; Hubbell, J. A. *Biomacromolecules* **2002**, *3*, 710−723.
(25) Gobin, A. S.; West, J. L. *FASEB J.* **2002**, *16*, 751−753.
(26) Lutolf, M. P.; Raeber, G. P.; Zisch, A. H.; Tirelli, N.; Hubbell, J. A. *Adv. Mater.* **2003**, *15*, 888−892.
(27) Lutolf, M. R.; Weber, F. E.; Schmoekel, H. G.; Schense, J. C.; Kohler, T.; Muller, R.; Hubbell, J. A. *Nat. Biotechnol.* **2003**, *21*, 513−518.
(28) Zisch, A. H.; Lutolf, M. P.; Ehrbar, M.; Raeber, G. P.; Rizzi, S. C.; Davies, N.; Schmoekel, H. G.; Bezuidenhout, D.; Djonov, V.; Zilla, P.; Hubbell, J. A. *FASEB J.* **2003**, *17*, 2260−2262.
(29) Lutolf, M. P.; Hubbell, J. A. *Biomacromolecules* **2003**, *4*, 713−722.
(30) Lutolf, M. P.; Lauer-Fields, J. L.; Schmoekel, H. G.; Metters, A. T.; Weber, F. E.; Fields, G. B.; Hubbell, J. A. *Proc. Natl. Acad. Sci. U.S.A.* **2003**, *100*, 5413−5418.
(31) Pratt, A. B.; Weber, F. E.; Schmoekel, H. G.; Muller, R.; Hubbell, J. A. *Biotechnol. Bioeng.* **2004**, *86*, 27−36.
(32) Rizzi, S. C.; Hubbell, J. A. *Biomacromolecules* **2005**, *6*, 1226−1238.
(33) Cappello, J. *Curr. Opini. Struct. Biol.* **1992**, *2*, 582−586.
(34) Yu, S. M.; Conticello, V. P.; Zhang, G.; Kayser, C.; Fournier, M. J.; Mason, T. L.; Tirrell, D. A. *Nature* **1997**, *389*, 167−170.
(35) Petka, W. A.; Harden, J. L.; McGrath, K. P.; Wirtz, D.; Tirrell, D. A. *Science* **1998**, *281*, 389−392.
(36) Cappello, J.; Crissman, J. W.; Crissman, M.; Ferrari, F. A.; Textor, G.; Wallis, O.; Whitledge, J. R.; Zhou, X.; Burman, D.; Aukerman, L.; Stedronsky, E. R. *J. Controlled Release* **1998**, *53*, 105−117.
(37) Heslot, H. *Biochimie* **1998**, *80*, 19−31.
(38) Panitch, A.; Yamaoka, T.; Fournier, M. J.; Mason, T. L.; Tirrell, D. A. *Macromolecules* **1999**, *32*, 1701−1703.
(39) Welsh, E. R.; Tirrell, D. A. *Biomacromolecules* **2000**, *1*, 23−30.
(40) Liu, C. Y.; Apuzzo, M. L. J.; Tirrell, D. A. *Neurosurgery* **2003**, *52*, 1154−1165.
(41) Heilshorn, S. C.; DiZio, K. A.; Welsh, E. R.; Tirrell, D. A. *Biomaterials* **2003**, *24*, 4245−4252.
(42) Maskarinec, S. A.; Tirrell, D. A. *Curr. Opin. Biotechnol.* **2005**, *16*, 422−426.
(43) Friedman, M.; Cavins, J. F.; Wall, J. S. *J. Am. Chem. Soc.* **1965**, *87*, 3672−3682.
(44) Lutolf, M. P.; Tirelli, N.; Cerritelli, S.; Cavalli, L.; Hubbell, J. A. *Bioconjugate Chem.* **2001**, *12*, 1051−1056.
(45) Prodromou, C.; Pearl, L. H. *Protein Eng.* **1992**, *5*, 827−829.
(46) Weber, F. E.; Eyrich, G.; Gratz, K. W.; Maly, F. E.; Sailer, H. F. *Int. J. Oral Maxillofac. Surg.* **2002**, *31*, 60−65.
(47) Weber, F. E.; Eyrich, G.; Gratz, K. W.; Thomas, R. M.; Maly, F. E.; Sailer, H. F. *Biochem. Biophys. Res. Commun.* **2001**, *286*, 554−558.
(48) Metters, A. T.; Anseth, K. S.; Bowman, C. N. *Polymer* **2000**, *41*, 3993−4004.
(49) Aumailley, M.; Gurrath, M.; Muller, G.; Calvete, J.; Timpl, R.; Kessler, H. *FEBS Lett.* **1991**, *291*, 50−54.
(50) Gurrath, M.; Muller, G.; Kessler, H.; Aumailley, M.; Timpl, R. *Eur. J. Biochem.* **1992**, *210*, 911−921.
(51) Bunch, T. A.; Brower, D. L. *Development* **1992**, *116*, 239−247.
(52) Aota, S.; Nomizu, M.; Yamada, K. M. *J. Biol. Chem.* **1994**, *269*, 24756−24761.
(53) Gauer, S.; SchulzeLohoff, E.; Schleicher, E.; Sterzel, R. B. *Eur. J. Cell Biol.* **1996**, *70*, 233−242.
(54) Felsenfeld, D. P.; Choquet, D.; Sheetz, M. P. *Nature* **1996**, *383*, 438−440.
(55) Watanabe, Y.; Dvorak, H. F. *Exp. Cell Res.* **1997**, *233*, 340−349.
(56) McDevitt, T. C.; Nelson, K. E.; Stayton, P. S. *Biotechnol. Prog.* **1999**, *15*, 391−396.
(57) Palecek, S. P.; Loftus, J. C.; Ginsberg, M. H.; Lauffenburger, D. A.; Horwitz, A. F. *Nature* **1997**, *385*, 537−540.
(58) Sheetz, M. P.; Felsenfeld, D. P.; Galbraith, C. G. *Trends Cell Biol.* **1998**, *8*, 51−54.
(59) Raeber, G. P.; Lutolf, M. P.; Hubbell, J. A. *Biophys. J.* **2005**, *89*, 1374−1388.
(60) Wolf, K.; Mazo, I.; Leung, H.; Engelke, K.; von Andrian, U. H.; Deryugina, E. I.; Strongin, A. Y.; Brocker, E. B.; Friedl, P. *J. Cell Biol.* **2003**, *160*, 267−277.
(61) Nabeshima, K.; Inoue, T.; Shimao, Y.; Sameshima, T. *Pathol. Int.* **2002**, *52*, 255−264.
(62) Lorimier, S.; Gillery, P.; Hornebeck, W.; Chastang, F.; Laurent-Maquin, D.; Bouthors, S.; Droulle, C.; Potron, G.; Maquart, F. X. *J. Cell. Physiol.* **1996**, *168*, 188−198.
(63) Dejana, E.; Languino, L. R.; Polentarutti, N.; Balconi, G.; Ryckewaert, J. J.; Larrieu, M. J.; Donati, M. B.; Mantovani, A.; Marguerie, G. *J. Clin. Invest.* **1985**, *75*, 11−18.
(64) Knox, P.; Crooks, S.; Scaife, M. C.; Patel, S. *J. Cell. Physiol.* **1987**, *132*, 501−508.
(65) Hiraoka, N.; Allen, E.; Apel, I. J.; Gyetko, M. R.; Weiss, S. J. *Cell* **1998**, *95*, 365−377.
(66) Hotary, K. B.; Yana, I.; Sabeh, F.; Li, X. Y.; Holmbeck, K.; Birkedal-Hansen, H.; Allen, E. D.; Hiraoka, N.; Weiss, S. J. *J. Exp. Med.* **2002**, *195*, 295−308.
(67) Brown, L. F.; Lanir, N.; McDonagh, J.; Tognazzi, K.; Dvorak, A. M.; Dvorak, H. F. *Am. J. Pathol.* **1993**, *142*, 273−283.
(68) Schmoekel, H.; Schense, J. C.; Weber, F. E.; Grätz, K. W.; Gnägi, D.; Müller, R.; Hubbell, J. A. *J. Orthop. Res.* **2004**, *22*, 376−381.
(69) Scheufler, C.; Sebald, W.; Hulsmeyer, M. *J. Mol. Biol.* **1999**, *287*, 103−115.
(70) Morpurgo, M.; Veronese, F. M.; Kachensky, D.; Harris, J. M. *Bioconjugate Chem.* **1996**, *7*, 363−368.

BM060504A